NEP-A and NEP-B both contribute to nuclear pore formation in *Xenopus* eggs and oocytes

Georgia Salpingidou[1], Ryszard Rzepecki[1,2], Elena Kiseleva[3], Carol Lyon[4], Birgit Lane[4], Kasia Fusiek[1,2], Anja Golebiewska[1,2], Shoena Drummond[5], Terry Allen[5], Juliet A. Ellis[6], Carl Smythe[7], Martin W. Goldberg[1] and Christopher J. Hutchison[1,*]

[1]Integrative Cell Biology Laboratories, School of Biological and Biomedical Sciences, The University of Durham, South Road, Durham DH1 3LE, UK
[2]Laboratory of Nuclear Proteins, University of Wroclaw, Przybyszewskiego 63/77, 51–148 Wroclaw, Poland
[3]Department of Morphology and Function of Cell Structure, Institute of Cytology and Genetics, Russian Academy of Sciences, Novosibirk-90, 630090, Russia
[4]School of Life Sciences, University of Dundee, Dow Street, Dundee DD1 4HN, UK
[5]CRUK, Department of Structural Cell Biology, Paterson Institute for Cancer Research, Christie Hospital, Wilmslow Road, Manchester M20 9BX, UK
[6]The Randall Division of Cell and Molecular Biophysics, Kings College, New Hunts House, Guy's Campus, London SE1 1UL, UK
[7]Centre for Developmental Genetics, Department of Biomedical Sciences, University of Sheffield, Firth Court, Western Bank, Sheffield S10 2TN, UK

*Author for correspondence (e-mail: c.j.hutchison@durham.ac.uk)

Summary

In vertebrates, the nuclear envelope (NE) assembles and disassembles during mitosis. As the NE is a complex structure consisting of inner and outer membranes, nuclear pore complexes (NPCs) and the nuclear lamina, NE assembly must be a controlled and systematic process. In *Xenopus* egg extracts, NE assembly is mediated by two distinct membrane vesicle populations, termed NEP-A and NEP-B. Here, we re-investigate how these two membrane populations contribute to NPC assembly. In growing stage III *Xenopus* oocytes, NPC assembly intermediates are frequently observed. High concentrations of NPC assembly intermediates always correlate with fusion of vesicles into preformed membranes. In *Xenopus* egg extracts, two integral membrane proteins essential for NPC assembly, POM121 and NDC1, are exclusively associated with NEP-B membranes. By contrast, a third integral membrane protein associated with the NPCs, gp210, associates only with NEP-A membranes. During NE assembly, fusion between NEP-A and NEP-B led to the formation of fusion junctions at which >65% of assembling NPCs were located. To investigate how each membrane type contributes to NPC assembly, we preferentially limited NEP-A in NE assembly assays. We found that, by limiting the NEP-A contribution to the NE, partially formed NPCs were assembled in which protein components of the nucleoplasmic face were depleted or absent. Our data suggest that fusion between NEP-A and NEP-B membranes is essential for NPC assembly and that, in contrast to previous reports, both membranes contribute to NPC assembly.

Supplementary material available online at
http://jcs.biologists.org/cgi/content/full/121/5/706/DC1

Key words: Nuclear Envelope Assembly, Nuclear Pore Complexes, LAP2

Introduction

The nuclear envelope (NE) is the boundary between the nucleoplasm and the cytoplasm in eukaryotic cells and has important roles in gene regulation (Hutchison, 2002). The NE consists of inner and outer nuclear membranes (INM and ONM, respectively), nuclear pore complexes (NPCs) and the nuclear lamina (Gerace and Burke, 1988). The ONM is continuous with the rough endoplasmic reticulum (ER) and is functionally similar to that organelle. By contrast, the INM contains a subset of at least 67 integral membrane proteins (IMPs) that make it biochemically distinct from ER (Schirmer et al., 2003). Of these, the best characterised are the so-called LEM domain proteins including emerin, the LAP2 family and MAN-1 (Lin et al., 2000). The ONM and INM converge at the pore membrane, which is adjacent to NPCs and is also characterised by unique IMPs, namely gp210 and POM121 (Wozniak et al., 1989; Hallberg et al., 1993). The INM is stable during interphase because of interactions between its unique IMPs and both the nuclear lamina and peripheral chromatin (e.g. Worman et al., 1988; Foisner and Gerace, 1993; Ye and Worman, 1996) (reviewed by Gruenbaum et al., 2000; Burke and Ellenberg, 2002).

During mitosis, the NE breaks down and must be reassembled at late anaphase or telophase. Breakdown of the NE is catalysed by the cdc2–cyclin-B kinase complex (Kishimoto, 1999), although the precise mechanism by which the NE breaks down is the subject of debate. Based upon work performed in egg systems, NE breakdown (NEBD) has been proposed to be preceded by breakdown of the nuclear lamina, mediated by phosphorylation of the constituent proteins of the lamina, the lamins (Gerace and Blobel, 1980; Peter et al., 1990; Ward and Kirschner, 1990; Heald and McKeon, 1990). This is followed by phosphorylation of IMPs of the INM (Pfaller et al., 1991; Courvalin et al., 1992; Foisner and Gerace, 1993) and fragmentation of the nuclear membrane into biochemically and morphologically distinct vesicles and tubules (Vigers and Lohka, 1992; Buendia and Courvalin, 1997; Marshall and Wilson, 1997; Drummond et al., 1999). A four-stage model for NE reassembly from NEP vesicles involves initial binding of NEP vesicles to chromatin,

fusion of the vesicles into an ER-like network, enclosure of the chromatin and then NPC formation and NE expansion (Mattaj, 2004). In vitro and in vivo fusion events are regulated by the small GTPase Ran and importin β (Hetzer et al., 2002; Zhang and Clarke, 2001; Walther et al., 2003a; Harel et al., 2003; Ryan et al., 2007). In vitro, fusion occurs between two distinct NEP types: NEP-B, which binds initially to chromatin; and NEP-A, which is required for fusion (Vigers and Lohka, 1991; Drummond et al., 1999).

NPCs are some of the most important structures in the NE. How NPC assembly is linked to NE assembly is still unclear. NPC assembly seems to occur in distinct steps. Pre-pore assembly, characterised by the presence of the Nup107-Nup160 complex occurs before, and independently of, NE assembly (Sheehan et al., 1988; Walther et al., 2003b). The binding of the Nup107-Nup160 complex to the chromatin is dependent on MEL-28/ELYS (Franz et al., 2007). This apparently is followed by early recruitment of the pore membrane protein POM121 and later recruitment of gp210. Moreover, while POM121 might be necessary for membrane fusion and pore assembly, gp210 appears to be largely dispensable (Bodoor et al., 1999; Antonin et al., 2005), although the role of gp210 is still the subject of debate (Drummond and Wilson, 2002). Recently, RNAi experiments have indicated that POM121 might also not be essential for NPC assembly, even in the absence of gp210 (Stavru et al., 2006a). A third integral membrane nucleoporin, NDC1, is essential for assembly of NPCs in human cells (Mansfeld et al., 2006), although *Caenorhabditis elegans* can survive through the process of development without NDC1 (Stavru et al., 2006b).

As indicated above, while the roles of individual membrane proteins in NPC assembly have been documented, it is unclear how NE assembly events per se affect NPC assembly. It had been implied, but not demonstrated, that only NEP-B vesicles contribute to NPC assembly (Vigers and Lohka, 1992), However, the findings of Antonin et al. support the hypothesis that the involvement of two distinct membrane populations contributes to assembly of not only the NE but also the NPC, and this might be achieved by segregating membrane proteins involved in NPC assembly at an early stage. Here, we show that gp210 is indeed segregated from POM121 and NDC1. gp210 is located exclusively in NEP-A membranes, whereas POM121 and NDC1 are located in NEP-B. Moreover, fusion between NEP-A and NEP-B promotes NPC assembly. Unexpectedly, by limiting the NEP-A contribution to the assembling NE, NPC products lacking components of the nucleoplasmic face are assembled. Taken together, these data show that NEP-A and NEP-B membranes both have essential roles in NPC assembly.

Results

Characterisation of novel IMPs of NEP-A and NEP-B vesicles

To investigate the properties and function of NEP-A and NEP-B vesicles, three new antibody reagents were generated against IMPs of the ER and NE. A polyclonal antibody against *Xenopus* lamina-associated polypeptide 2 (XLAP2) detected a ~68-kDa protein in extracts of *Xenopus* tissue culture (XTC) cell lines and decorated the NE in fixed cells (Fig. 1a,b). The antibody also detected polypeptides of ~84 kDa and 40 kDa in *Xenopus* egg extracts (Fig. 1a). These findings are consistent with the LAP2 polypeptides previously reported to be differentially expressed in *Xenopus* eggs, embryos and somatic cells (Lang et al., 1999). Monoclonal antibodies CEL13A and CEL1FF were generated from mice that were immunised with sperm pronuclei assembled in *Xenopus* egg extracts. Both antibodies decorated the NE of germinal vesicles (GVs) of stage IV *Xenopus* oocytes (data not shown; see also C. Lyon, Immunological studies of the molecular basis of nuclear envelope structure and function, PhD thesis, University of Dundee, 1995) and detected proteins of 40.2 kDa and 30.1 kDa, respectively, in *Xenopus* egg extracts. Finally, the monoclonal antibody LAP12 (Harris et al., 1994) detected a 36.3 kDa protein in *Xenopus* egg extracts (data not shown).

To investigate the distribution of each protein between different membranes, NEP-A, NEP-B and cytosolic fractions of *Xenopus* egg extracts were prepared as described previously (Vigers and Lohka, 1991; Drummond et al., 1999). To verify that the procedure yielded discrete fractions, SDS-PAGE and staining with Coomassie Blue was performed (Fig. 1c). The fractions were then used for immunoblotting with each antibody reagent in order to determine the relative distribution of the antigens. As a control, blots were probed with antibody CEL5C, which was shown previously to be distributed equally between NEP-A and NEP-B (Drummond et al., 1999). As expected CEL5C detected a single band of ~66 kDa in both NEP-A and NEP-B but did not react with cytosol. The CEL13A antigen and the LAP12 antigen were both preferentially located in NEP-A vesicles, although small amounts were detected in NEP-B. By contrast, the CEL1FF antigen and the XLAP2 polypeptides were located almost exclusively in NEP-B vesicles, with only small amounts detected in NEP-A and none in the cytosol (Fig. 1d). Including the NEP-A and NEP-B reagents described previously [*Xenopus* lamin B receptor (xLBR) and anti-NEP-B78 (Drummond et al., 1999)], this panel of reagents provided us with three antibodies specific for NEP-A, three antibodies specific for NEP-B and one antibody that detected antigens in both vesicle populations. Based upon our previous nomenclature, we referred
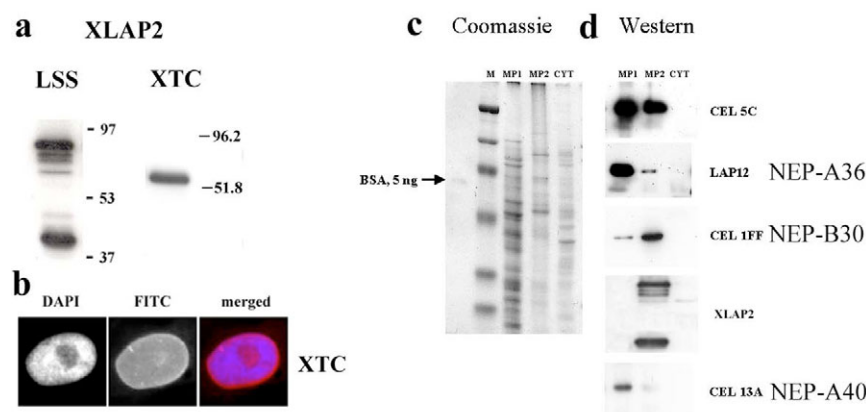

Fig. 1. Characterisation of novel markers of NEP-A and NEP-B. (a) Affinity-purified antisera against XLAP2 were used to immunoblot *Xenopus* egg extracts (LSS) or cell extracts from *Xenopus* tissue culture cells (XTCs). Molecular mass standards are shown to the right of each blot. (b) Alternatively, XTC cells were prepared for immunofluorescence and stained with antibody against XLAP2 followed by TRITC-labelled goat anti-rabbit antibody and counter stained with DAPI. (c,d) NEP-A, NEP-B and membrane-free cytosol were resolved by 10% SDS-PAGE and either stained with Coomassie Blue (panel c) or immunoblotted (panel d) for the presence of CEL5C, CEL13A, LAP12, CEL1FF or XLAP2. M, molecular weight markers; MP1, NEP-A vesicles; MP2, NEP-B vesicles; CYT, membrane-free cytosol.

to the antigens detected by CEL1FF, CEL13A and LAP12 as NEP-B30, NEP-A40 and NEP-A36, respectively.

XLAP2 has been characterised previously as an IMP (Lang et al., 1999). To characterise the new antigens further, total membrane fractions from *Xenopus* egg extracts were subjected to extraction with salts, urea or detergents, as described previously (Drummond et al., 1999). All three antigens behaved as IMPs (supplementary material Fig. S1).

We have also reported previously that NEP-B is detected in the NE of sperm pronuclei assembled in unfractionated *Xenopus* egg extracts ~15 minutes earlier than NEP-A vesicles (Drummond et al., 1999). To investigate the timing of incorporation of the new NEP-A and NEP-B antigens into sperm pronuclei assembled in vitro, we performed immunofluorescence on assembling nuclei in *Xenopus* egg extracts. We found that all antigens present in NEP-B (NEP-B78, NEP-B30 and XLAP2; see supplementary material Fig. S2a-c) were first detected in the assembling NE ten minutes before NEP-A40 (supplementary material Fig. S2d) and xLBR [data not shown, but see Drummond et al. (Drummond et al., 1999)], indicating that the new antibody

reagents were accurate discriminators of NEP-A and NEP-B behaviour.

The new data identify five new NEP-A and NEP-B proteins. Although, with the exception of XLAP2, we do not yet know the function of these proteins, here their presence is used as biomarkers to distinguish between NEP-A and NEP-B in various assays.

Fusion of vesicles containing NEP-A antigens to the growing NE of stage III oocytes correlates with NPC assembly

In order to investigate the relevance of vesicle fusion to NE assembly in vivo, we used field-emission scanning electron microscopy (feSEM) and thin-section transmission electron microscopy (TEM) analysis of whole isolated *Xenopus* oocyte GV NEs. *Xenopus* oocytes develop over a period of approximately six months. During this period, the oocytes undergo an approximate tenfold increase in volume, with the GVs undergoing similar increases in size. Thus, in stage II-IV oocytes, one would expect massive expansion of the NE (Dumont, 1972; Smith et al., 1991) and therefore expect assembly processes to occur. Therefore, we
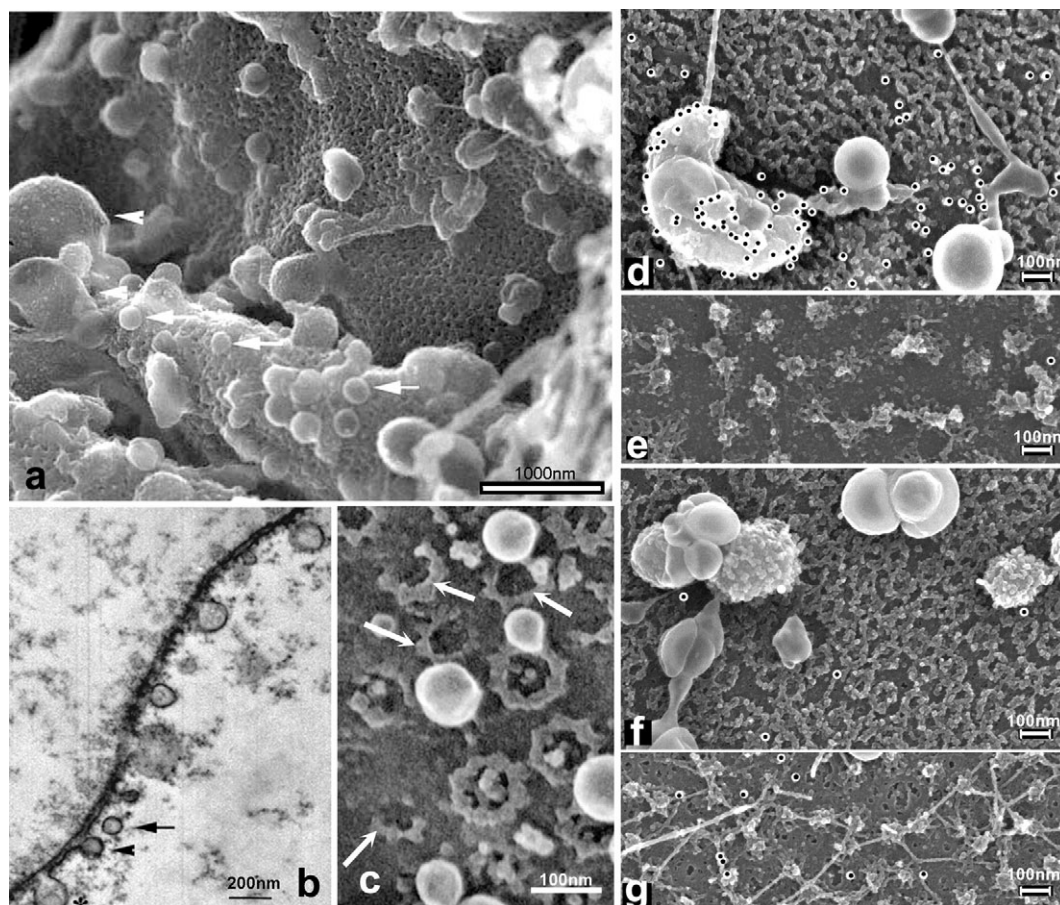

Fig. 2. Association of membrane vesicles with manually isolated stage III-IV GV envelopes. Whole GVs were manually isolated from stage III-IV *Xenopus* oocytes and prepared for either feSEM microscopy (a,c) or thin-section TEM (b). Arrowheads show large vesicles and arrows show small smooth vesicles in panel a. In thin-section TEM, vesicles that were close to (arrow), attached to (arrowheads) or fused with the ONM (*) are shown in panel b. NPC intermediates (arrowheads) that appear at high density in the vicinity of areas of membrane fusion are illustrated in panel c. Samples were prepared for immunogold labelling with either CEL13A (NEP-A, panels d,e) or antibody against XLAP2 (NEP-B, panels f,g). Panels d and f show the ONM, whereas panels e and g show the INM. In the micrographs, individual gold particles (appearing black) have been artificially highlighted with white rings to improve their visibility. CEL13A decorated a range of vesicles varying in diameter from 100–500 nm, as well as the ONM. Antibodies against XLAP2 decorated the INM and to some extent the ONM but did not decorate any of the vesicles. Bars, 1000 nm (a); 200 nm (b); 100 nm (c-g).

anticipated that stage II-III oocyte GVs would provide an in vivo model for NE growth and assembly. Using feSEM, we observed that GVs isolated from stage II–III oocytes were covered in membrane vesicles (Fig. 2a). The vesicles ranged in size from significantly larger than NPCs (Fig. 2a, arrowheads) to vesicles of the same size as NPCs (Fig. 2a, arrows). As fusion is not inhibited in these assays, it is difficult to correlate these sizes directly with isolated NEP vesicles; however, the majority of small vesicles range in size from ~50–400 nm in diameter, whereas larger vesicles were between 600–800 nm in diameter. This is entirely consistent with the dimensions of biochemically fractionated NEP vesicles, which previously have been estimated as varying in size between 100–800 nm in diameter (Drummond et al., 1999). Complementary results were obtained by thin-section TEM. Three 'modes' of vesicle behaviour were observed. Some vesicles were always fused with the ONM (Fig. 2b, asterisk), whereas other vesicles appeared to be either close to, but not in contact with, the ONM (Fig. 2b, arrow) or docked to but not fused with the ONM (Fig. 2b, arrowhead; note that vesicles observed by TEM varied from 100–200 nm in diameter, but it is difficult to correlate these directly with vesicles observed by SEM owing to differences in sample preparation). Using feSEM, we observed that areas of NE containing high densities of vesicles also contained high densities of partially assembled NPC intermediates (Goldberg et al., 1997) (Fig. 2c,

arrows). To attempt to identify the vesicles, we used antibodies against NEP-A and NEP-B components for immunogold labelling. Antibody against NEPA40 readily detected the majority of vesicles on the ONM (Fig. 2d) as well as the ONM itself but was almost absent from the INM (Fig. 2e). Some small vesicles (diameter <200 nm) were only slightly labelled. By contrast, antibodies against XLAP2 decorated the INM extensively (Fig. 2g) and, to some extent, the ONM. However, none of the vesicles was decorated by antibody against XLAP2. One interpretation of these data is that NE growth in stage III oocytes is characterised by continued fusion of NEP-A vesicles into preformed membranes containing NEP-A and NEP-B proteins but with little additional fusion of NEP-B membranes. However, the most significant finding is that, where vesicle fusion occurs, a high frequency of NPC assembly intermediates is observed.

NPC assembly occurs at the fusion boundary between NEP-A and NEP-B vesicles

Because GV assembly is difficult to manipulate experimentally, we decided to use fractionated extracts of *Xenopus* eggs to investigate further the relationship between NEP-A fusion and NPC assembly. Egg extracts were fractionated to generate NEP-A, NEP-B and membrane-free cytosol (Drummond et al., 1999). Sperm chromatin was preincubated in cytosol containing NEP-B.
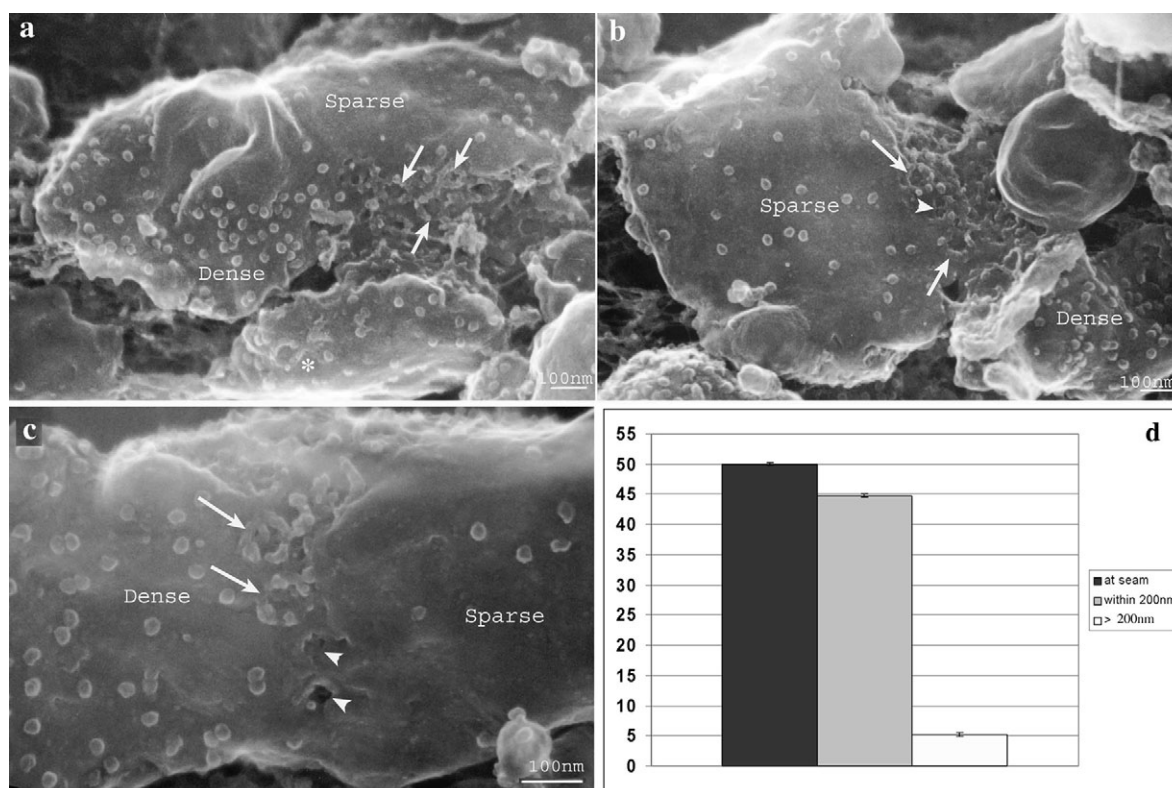

Fig. 3. NPCs form at boundaries between rough and smooth membranes. Sperm chromatin was preincubated with NEP-B and cytosol before addition of NEP-A. Assembling sperm pronuclei were isolated and prepared for feSEM microscopy. (a-c) Each micrograph shows examples of the morphology of fusing vesicles observed five minutes after addition of NEP-A. At very high frequency, membranes with dense concentrations of ribosomes (labelled 'dense') can be seen to be joined to membranes with sparse concentrations of ribosomes ('sparse'), and these are interpreted as initial fusion boundaries between single NEP-A and NEP-B vesicles. NPCs (arrows) and NPC assembly intermediates (arrowheads) were observed at the boundaries between dense and sparse areas of membranes. Bars, 100 nm. (d) Quantification of the position of NPC assembly was performed by measuring the distance from the nearest fusion seam of >300 randomly selected NPC intermediates in three independent experiments. The graph shows the percentage of NPC intermediates that were either at a fusion seam, within 200 μm of a fusion seam or >200 μm from a fusion seam. Bars, ±s.e.m.
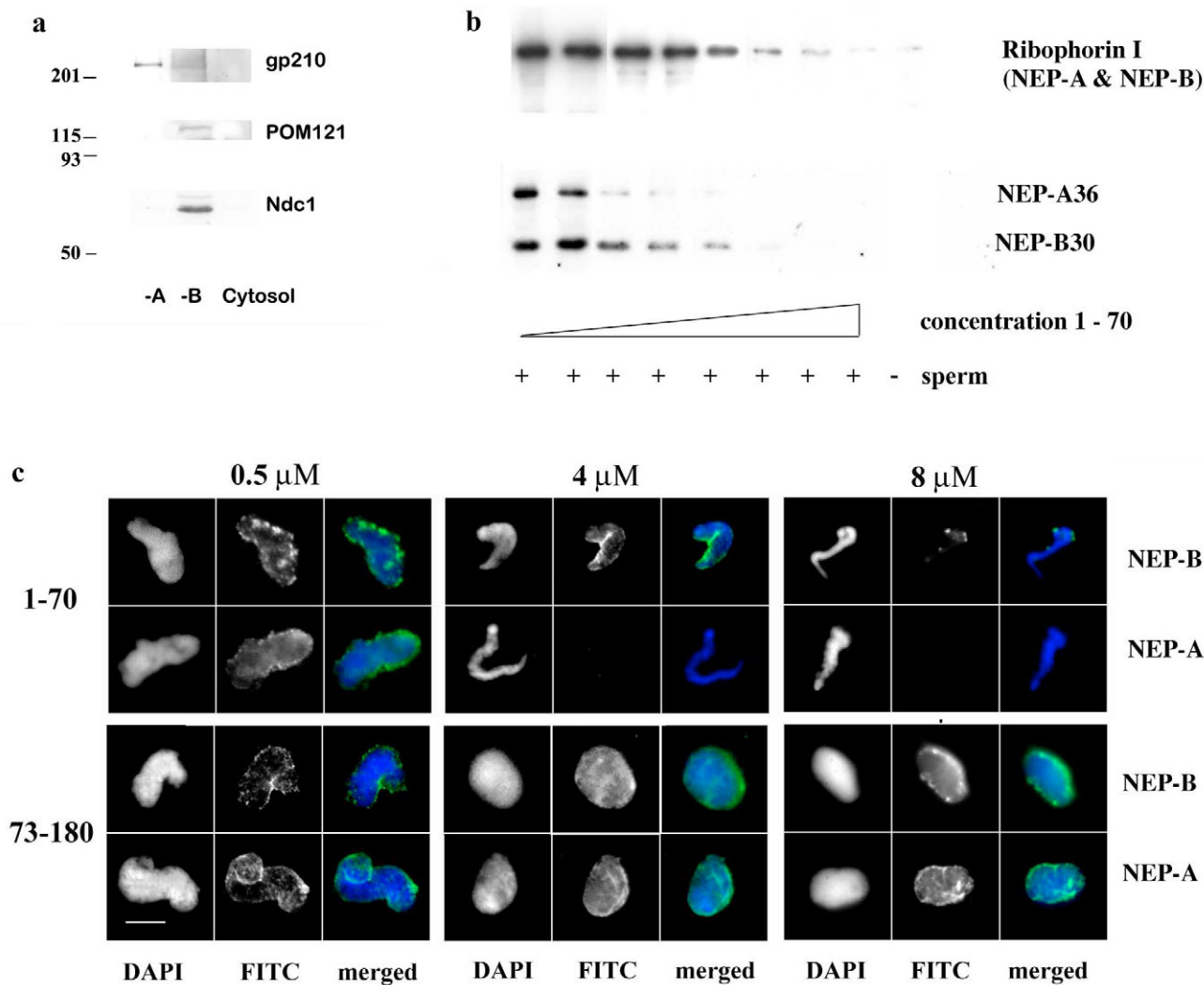
Fig. 4. Inhibition of NE assembly by human emerin constructs. (a) NEP-A (labelled '-A'), NEP-B (labelled '-B') and cytosol were immunoblotted with antibodies against gp210, POM121. Molecular mass markers are indicated on the left-hand side. (b,c) Human emerin peptides 1-70 or 73-180 were added to *Xenopus* egg extracts at concentrations ranging from 0.5 μM to 8.0 μM. The ability of extracts to assemble sperm pronuclei in the presence of each peptide was assessed by either immunoblotting assays (b) or immunofluorescence assays (c). Here, mAb 4G12 was used to detect NEP-B and mAb CEL13A was used to detect NEP-A in immunofluorescence assays, whereas CEL1FF was used to detect NEP-B, and LAP12 was used to detect NEP-A in immunoblotting assays. CEL5C was used to detect total membranes. Bar, 10 μm.

NEP-A was then added, and assembling sperm pronuclei were recovered at two-minute intervals and prepared for feSEM. Approximately five minutes after addition of NEP-A, evidence of vesicle fusion between individual NEP-A and NEP-B vesicles could be observed as membranes with relatively dense concentrations of ribosomes (NEP-A) were joined to membranes with relatively sparse concentrations of ribosomes (NEP-B; Fig. 3a-d). A boundary between these areas was clearly visible, and, at these boundaries, large numbers of either fully formed NPCs (Fig. 3a-c, arrows) or NPC assembly intermediates (Fig. 3b,d, arrowheads) were always observed. Indeed, at these very early stages of NE assembly, 50% of NPCs and NPC intermediates were observed directly at fusion boundaries, 44.8% within 200 nm of the boundaries, whereas only 5.2% were observed at a distance greater than 200 nm from the boundaries (Fig. 3d). These data suggested that the initial fusion between NEP-A and NEP-B vesicles promoted NPC assembly.

NEP-A and NEP-B contain different pore membrane proteins and are both required for correct assembly of NPCs

To understand why fusion between NEP-A and NEP-B might promote NPC assembly, we first investigated the distribution of the pore membrane proteins POM121 and gp210 as well as the IMP NDC1 with NEP fractions by immunoblotting. We found that gp210 was almost exclusively associated with NEP-A, whilst POM121 and NDC1 were found exclusively in NEP-B (Fig. 4a). To determine how fusion between NEP-A and NEP-B might contribute to NPC assembly, we used LEM domain peptides from human emerin to interfere with NEP chromatin binding. Previous studies had revealed that truncation mutants of LAP2, corresponding to the LEM domain, have profound influences on NE assembly (Gant et al., 1999). We reasoned that, because NEP-A and NEP-B contained apparently different complements of LEM domain proteins, their binding to chromatin might be differentially sensitive to the presence of LEM domain peptides. Sequences encoding peptides
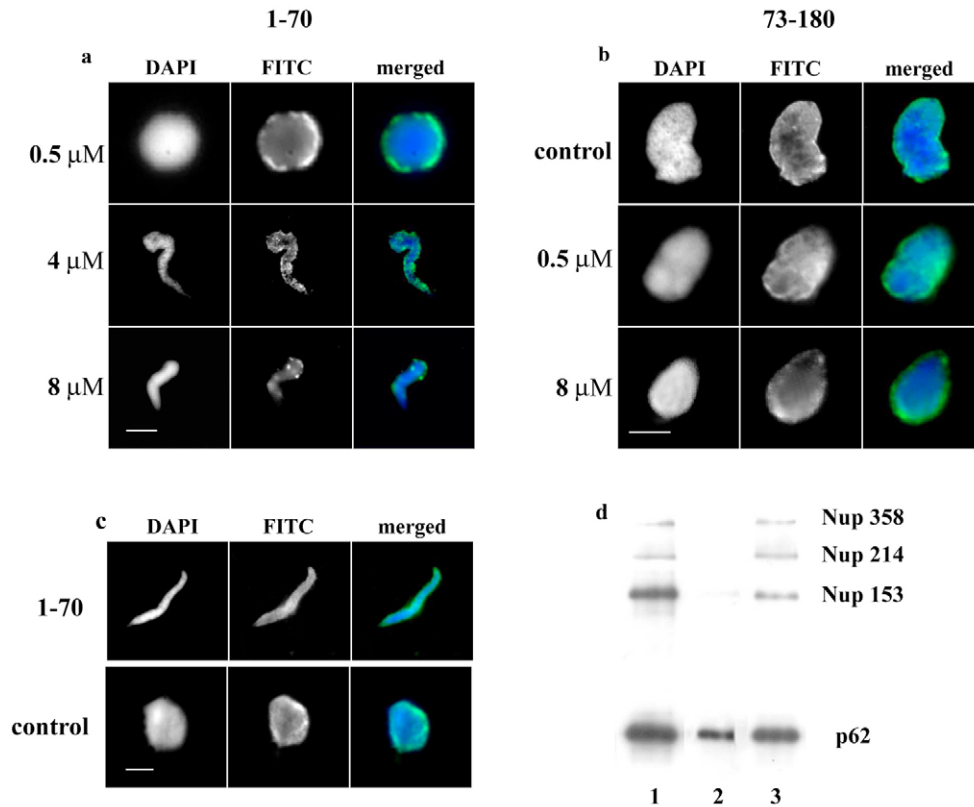
Fig. 5. Inhibition of NPC assembly by human emerin constructs. Human emerin peptides 1-70 (a,c) and 73-180 (b) were added to *Xenopus* egg extracts at concentrations between 0.5 and 8.0 μM. Alternatively, no peptides were added to extracts in order to measure normal assembly (labelled 'control' in b,c). The effects of the peptides on NPC assembly were investigated by immunofluorescence using antibodies against FG-repeat nucleoporins (a,b) or Nup107 (c). Bars, 10 μm. (d) Alternatively, nuclei were assembled in extracts containing 4.0 μM peptide 73-180 (lane 1) or peptide 1-70 (lane 3). Nuclei were isolated and prepared for immunoblotting using antibodies against FG-repeat nucleoporins. Lane 2 contains material recovered from extracts containing no nuclei.

corresponding to either the LEM domain and LEM shadow domain of emerin (residues 1-70) or as a control the lamin-A-binding domain of emerin (residues 73-180) were cloned as His-tagged sequences expressed in *Escherichia coli* and purified (supplementary material Fig. S3a,b). Both peptides were able to bind to decondensed but not condensed chromatin (supplementary material Fig. S3c). To determine the influence of each peptide on NE assembly in unfractionated egg extracts, the peptides were added at increasing concentrations, and NE assembly was monitored by either immunofluorescence or immunoblotting. At concentrations of 0.5 μM, neither peptide affected NE assembly. At a concentration of 4 μM, the LEM domain peptide inhibited sperm decondensation. At this concentration, NEP-B was still bound to chromatin. By contrast, NEP-A was largely absent, as determined by immunofluorescence, although immunoblotting revealed that some NEP-A remained associated with chromatin (Fig. 4b,c). At higher concentrations (8 μM), all NEP binding was inhibited (Fig. 4b). The peptide corresponding to the lamin-A-binding domain did not influence NE assembly or chromatin remodelling at concentrations of up to 8.0 μM (Fig. 4b).

To investigate the possibility that NEP-A and NEP-B both contribute to NPC assembly, we investigated NPC assembly in sperm pronuclei assembled in the presence of emerin peptides. As expected, the assembly of FG-repeat nucleoporins (as judged by immunostaining with mAb 414) was not affected by peptide 73-180 (Fig. 5b). By contrast, peptides 1-70 (Fig. 4a) progressively inhibited the association of FG-repeat nucleoporins with chromatin in a way that was reminiscent of the inhibition of NEP-B vesicle binding. At a concentration of 4.0 μM, there was significant staining of the nuclear periphery with mAb 414 (Fig. 5a). However, at 8.0 μM, mAb 414 staining was significantly depleted (data not shown).

To investigate further how interference of NEP-A and NEP-B binding influenced NPC assembly, we used a polyclonal antibody against Nup107 to investigate the assembly of pre-pore complexes (Walther et al., 2003b). Even when used at a concentration of 8.0 μM (a concentration that inhibits NEP-B vesicle binding to chromatin), none of the peptides prevented the association of Nup107 with sperm chromatin (Fig. 5c). This result indicated that the assembly of pre-pore complexes was unaffected by the absence of NEP-A and NEP-B vesicles or indeed the presence of emerin peptides.

To gain additional insight into how perturbing the balance between NEP-A and NEP-B binding and fusion influences NPC assembly, sperm pronuclei assembled in the presence of peptides 1–70 and 73-180 at a concentration of 4.0 μM were isolated and used for immunoblotting. We found that some FG-repeat nucleoporins were equally abundant in the presence of both peptides (Nup214 and Nup358). By contrast, other FG-repeat nucleoporins were depleted significantly (p62 by ~75% and Nup153 by ~80%; Fig. 5d) in the presence of peptide 1-70. These data suggested that, by limiting the contribution of NEP-A to NE assembly, FG-repeat nucleoporins associated with the cytoplasmic face of the NPC are relatively unaffected, whereas FG-repeat nucleoporins associated with the central transporter and nucleoplasmic face of NPCs are depleted. To confirm this finding, we performed immunofluorescence on nuclei assembled in the presence of emerin peptides with antibodies specific for either Nup153 or Nup214 (Fig. 6). Nuclei assembled in the presence of peptide 73-180 were stained as brightly as controls with both antibodies. By contrast, nuclei assembled in the presence of peptide 1-70 were barely stained with antibodies against Nup153 but were stained brightly with antibodies against Nup214. These findings confirmed that nuclei assembled

in the presence of LEM domain peptides were relatively depleted of nucleoporins located at the INM. To confirm that the depletion of nucleoporins resulted from depletion of NEP-A (as opposed to the presence of the peptides), fractionated extracts were reconstituted with either normal amounts of NEP-A or with a tenfold reduction in the amount of NEP-A. Nuclei assembled in NEP-A-depleted extracts contained levels of Nup358 and Nup214 similar to those of controls (as judged by immunofluorescence and immunoblotting; Fig. 7a,c,d). By contrast, the level of Nup153 was reduced by >70% (Fig. 7b,d), showing that depletion of NEP-A consistently results in depletion of nucleoporins located at the INM.

To investigate this finding further, we assembled nuclei in the presence of emerin peptides at a concentration of 4.0 μM and used feSEM to investigate the morphology of the ONM and NPCs. In controls and in the presence of peptide 73–180 (Fig. 8a-d), sperm pronuclei were assembled that had well-distributed NPCs (white circles) and that were covered with ribosomes (arrows). By contrast, in the presence of peptides 1–70 (Fig. 8e,f), the NE appeared completely abnormal. Very few ribosome-like structures were observed, confirming that NEP-A is substantially depleted. By contrast, in some areas, very high densities of structures that resembled the outer ring of the NPC could be seen. While some of these structures looked complete (Fig. 8f, white circles), most appeared only partially assembled and were clustered together (black circles). Taken together, these findings suggest that depletion of NEP-A, relative to NEP-B, perturbs the assembly of NPCs.

Discussion

Fusion of NEP-A and NEP-B correlates with NPC assembly

In this investigation, we have generated novel antibody and peptide reagents that we have used to investigate the assembly of the NE and NPC in vivo and in vitro in *Xenopus* eggs and oocytes. In stage III oocytes, growth of the GV is characterised by extensive fusion of vesicles containing NEP-A IMPs into a NE containing both NEP-A and NEP-B IMPs. Where extensive fusion of this type occurs, structures resembling NPC assembly intermediates (Goldberg et al., 1997) are always observed. In fractionated extracts of *Xenopus* eggs, reconstitution of NEP-A and NEP-B leads to very early fusion events between the two membrane types. As NEP-A and NEP-B are morphologically distinct [NEP-A is covered with ribosomes, whereas NEP-B is smooth (Drummond et al., 1999)], fusion between the two membranes can be readily observed, and fusion boundaries are characterised by the assembly of NPCs and NPC intermediates. These two findings suggest that fusion of NEP-A with NEP-B promotes the assembly of NPCs.

Recent reports have shown that NPC assembly begins with the recruitment of a pre-pore complex termed the Nup107–Nup160 complex to chromatin. Recruitment of this complex is dispensable for membrane binding and fusion but is necessary for downstream recruitment of FG-repeat nucleoporins (Walther et al., 2003b). Our current data extend these findings as disruption of NEP binding to chromatin does not influence assembly of the pre-pore complex, suggesting that, at very early stages of NE assembly, NEP-B binding and pre-pore binding to chromatin are completely independent of each other. Subsequently, further assembly of NPCs is dependent upon recruitment of components of the pore membrane. We show here that the pore membrane proteins gp210 and POM121 are segregated between the two NEP fractions, with gp210 residing in NEP-A and POM121 in NEP-B. Moreover, the integral membrane
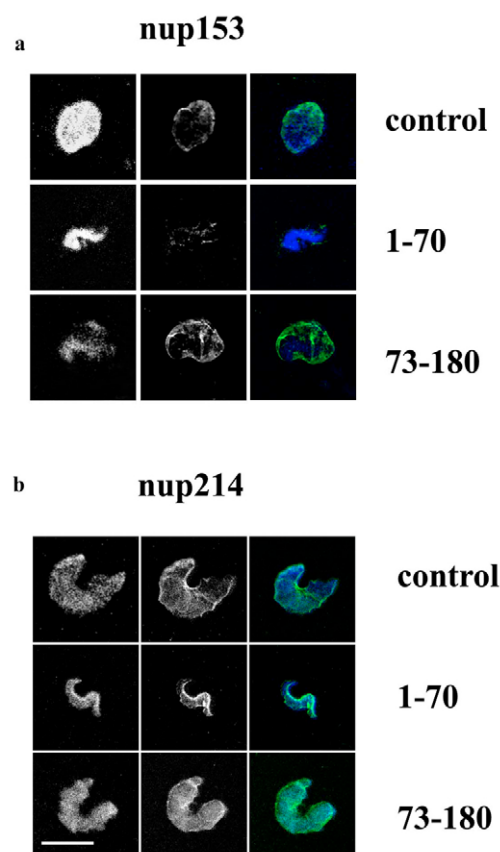

Fig. 6. Preferential depletion of Nup153 in nuclei assembled in the presence of peptide 1-70. Nuclei were assembled in egg extracts containing 4.0 μM peptides 1-70 or 73-180 and prepared for immunofluorescence. Nuclei were stained with antibodies against Nup153 (a) or Nup214 (b) followed by FITC-labelled goat anti-mouse antibody and counter stained with DAPI. Images are presented as mono images or two-colour merged images. Bar, 10 μm.

protein NDC1, which is essential for recruitment of soluble nucleoporins during NPC assembly (Mansfeld et al., 2006) is also located exclusively in NEP-B. This finding is entirely consistent with earlier reports that NDC1 co-segregates with POM121 (Mansfield et al., 2006).

One report has suggested that gp210 is recruited at a very early stage of NPC assembly and that inhibiting gp210 function inhibits close apposition of nuclear membranes and prevents NPC dilation by inhibiting the recruitment of Nup98, Nup153 and Nup214 but not p62 (Drummond and Wilson, 2002). In a more recent report, it has been suggested that pom121 and gp210 are recruited to forming NEs at different times. Pom121 was recruited at an early stage, whereas gp210 is recruited later (Antonin et al., 2005). This observation is consistent with an earlier publication that also suggested the occurrence of late recruitment of gp210 to forming NEs (Bodoor et al., 1999). Moreover, while depletion of Pom121 prevented NE fusion and NPC assembly in egg extracts, depletion of gp210 had little or no apparent effect on either NE assembly or the formation of NPCs (Antonin et al., 2005). RNAi knockdown of gp210 in *C. elegans* does cause clustering of NPCs and the accumulation of abnormal NPC intermediates (Cohen et al., 2003). At least some of the abnormal NPC intermediates described in the study (twinned membranes), as well as the clustering of NPCs implied
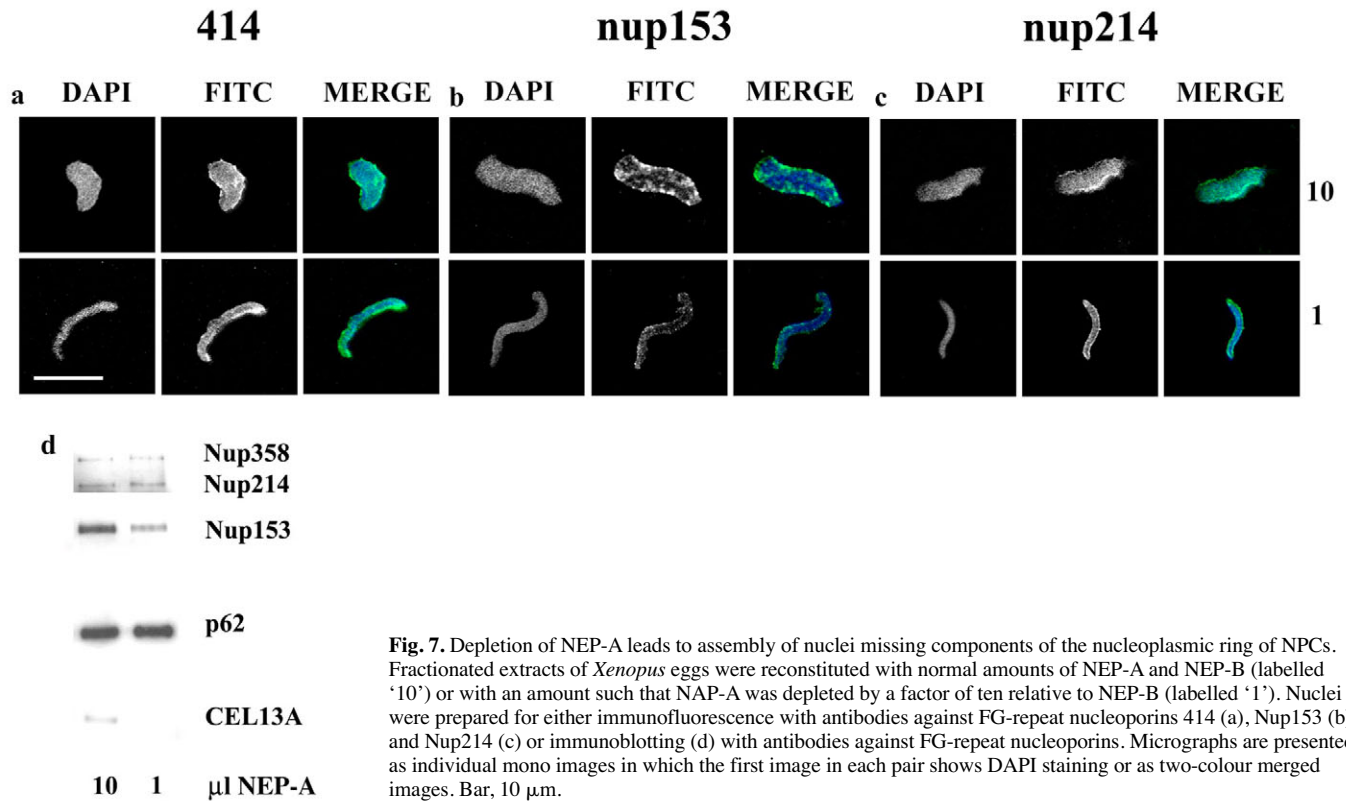
Fig. 7. Depletion of NEP-A leads to assembly of nuclei missing components of the nucleoplasmic ring of NPCs. Fractionated extracts of *Xenopus* eggs were reconstituted with normal amounts of NEP-A and NEP-B (labelled '10') or with an amount such that NAP-A was depleted by a factor of ten relative to NEP-B (labelled '1'). Nuclei were prepared for either immunofluorescence with antibodies against FG-repeat nucleoporins 414 (a), Nup153 (b) and Nup214 (c) or immunoblotting (d) with antibodies against FG-repeat nucleoporins. Micrographs are presented as individual mono images in which the first image in each pair shows DAPI staining or as two-colour merged images. Bar, 10 μm.

preferential depletion of nucleoplasmic structures (Cohen et al., 2003), and this is consistent with depletion of Nup153 (Drummond and Wilson, 2002). Our data can therefore be reconciled with the findings of Antonin and coworkers (Antonin et al., 2005), Bodoor and coworkers (Bodoor et al., 1999) and Cohen and coworkers (Cohen et al., 2003) but are more difficult, but not entirely impossible, to reconcile with the work of Drummond et al. (Drummond and Wilson, 2002). Pom121 appears early during NE assembly because it is a component of NEP-B vesicles, whereas the late assembly of gp210 reflects its association with NEP-A. A third integral membrane protein required for NPC assembly is NDC1, and this protein is also associated with NEP-B. RNAi-mediated knockdown of this protein in mammalian cells leads to defective downstream assembly of soluble nucleoporins Nup205, Nup93 and Nup53 (Mansfeld et al., 2006). Therefore, depletion of pom121, NDC1 or NEP-B would therefore be expected to have catastrophic effects on the further recruitment of FG-repeat nucleoporins, as reported by Antonin et al. (Antonin et al., 2005) and as shown here (Fig. 5). By contrast, depletion of gp210 has only partial effects on NPC assembly, as reported by Cohen and colleagues (Cohen et al., 2003), which might be restricted to preferential
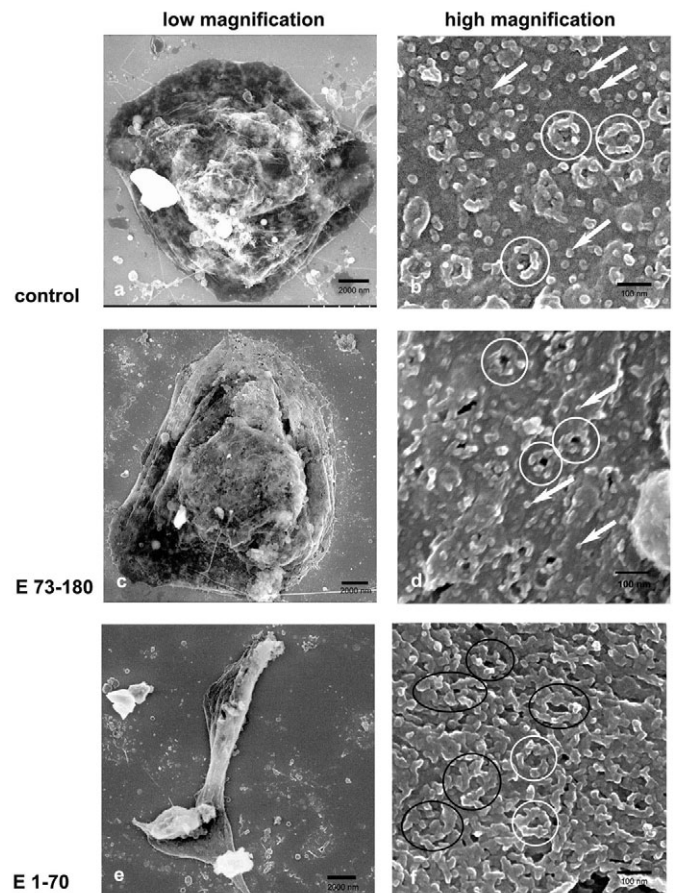

Fig. 8. Analysis by feSEM of NEs and NPCs assembled in the presence of emerin peptides. Sperm pronuclei were assembled in either the absence (labelled 'control' in a,b) or presence of 4.0 μM emerin peptide 73-180 (c,d) or emerin peptide 1-70 (e,f). Samples were prepared for feSEM microscopy and examined at either low (a,c,e) or high (b,d,f) magnification. Ribosomes are indicated by arrows. Apparently intact fully formed NPCs are indicated by white circles, but these are rare in panel f, where more-abnormal structures predominate (black circles). Bars, 2000 nm (a,c,e); 100 nm (b,d,f).

loss of nucleoplasmic ring structures. This is directly analogous to restricting the recruitment of NEP-A membranes to chromatin (as was performed in this study), which also leads to a preferential loss of nucleoplasmic nucleoporins and an accumulation of clustered and abnormally formed NPCs (Fig. 8). Our findings can therefore be reconciled with those of Antonin and coworkers as it can be argued that, in addition to restricting the amount of gp210 in the NE, by limiting the contribution of NEP-A, additional IMPs would also be depleted from the forming NE, thus further perturbing assembly of NPCs.

In our study, the most consistent effect of depleting NEP-A on NPC assembly was the loss of Nup153. Nup153 is a relatively late-assembly component of NPCs (Smythe et al., 2000) and is required for the assembly of the nuclear pore basket, interaction with the nuclear lamina and for anchorage of NPCs within the NE (Smythe et al., 2000; Walther et al., 2001). It is unclear from the current study whether depletion of Nup153 is caused directly through depletion of NEP-A or whether the pores that are assembled are transport incompetent and therefore in turn cannot import and assemble Nup153. Nevertheless, the partially assembled NPCs that were observed in NEP-A-depleted envelopes were clustered, which is a typical feature of pores lacking Nup153 (Walther et al., 2001).

Although it is clear that depletion of NEP-A would in turn restrict the amount of gp210 available for NPC assembly, given the contentious views of the role of gp210 in NPC assembly, we cannot at this time conclude that this depletion leads directly to abnormal assembly of NPCs. It is possible that as-yet-uncharacterised membrane proteins in NEP-A also participate in the assembly of NPCs, and this could be the focus of future work. However, taken together, our data show that NEP-A has a clear role in NPC assembly, which is initiated by the fusion of this vesicle population with NEP-B.

Materials and Methods

Antibody reagents
Antibodies against XLAP2 protein were raised in rabbits against a bacterially expressed and purified N-terminal fragment of XLAP2 amino acids 1-164. This region contains the LEM domain and the entire 'common domain' (if alternative splicing of the *XLAP2* transcript indeed takes place in *Xenopus*). Rabbit sera were affinity purified using XLAP2 1-164 protein covalently bound to sepharose columns (see also Rzepecki et al., 1998). The working dilution of antibody against XLAP2 was 1 in 100 to 1 in 200. Monoclonal antibodies CEL1FF and CEL13A were generated from spleenocytes obtained from mice immunised with sperm pronuclei assembled in vitro. Hybridomas were made as described previously (Harlow and Lane, 1996) and selected according to their ability to secrete antibodies that reacted with proteins extracted from sperm pronuclei and that decorated the NEs of oocyte GVs (C. Lyon, Immunological studies of the molecular basis of nuclear envelope structure and function, PhD thesis, University of Dundee, 1995). Both antibodies were used at working dilutions of 1 in 20 to 1 in 50. Monoclonal antibodies 4G12 and CEL5C have been described previously (Drummond et al., 1999). Mouse monoclonal LAP12 antibody was a kind gift from Roland Foisner, (Medical University of Vienna, Austria) and was used at a dilution of 1 in 100 to 1 in 200. Rabbit polyclonal antibody against Nup107 was a generous gift of Iain Mattaj (EMBL, Heidelberg, Germany) and was used at a dilution of 1 in 200.

DNA constructs
Plasmid DNAs pET29b emerin 1-176 and pET29b emerin 1-70, for emerin deletion mutants overexpressed in bacteria, were a kind gift from Juliet Ellis (Kings College London, UK). Plasmid pET 23a XLAP2 1-164 was a kind gift from Kathrin L. Wilson (Baltimore, MD). Plasmid pET29b emerin 73-180 was prepared using a PCR reaction with full-length cDNA for human emerin as a template and a combination of primers for the restriction sites created by *Nde*I or *Hin*dIII (forward) and *Sal*I (reverse). PCR products were digested with a full set of restriction enzymes and ligated after digestion in the same way as plasmid DNA. The following enzymes and primers were used: *Nde*I for the emerin73 forward reaction with pET29b: 5′-GCA CAT ATG TAT GAT CTT CC-3′; and *Sal*I for the emerin180 reverse reaction with pET29b and pEGFP-C1: 5′-AGG GTC GAC GGA CAG GTC CAG-3′.

Protein overexpression and purification
All proteins overexpressed in bacteria were fusion proteins containing a poly-histidine tag. All emerin proteins were expressed in bacteria as soluble proteins. All proteins overexpressed in bacteria were affinity purified on Ni-NTA-agarose beads to near homogeneity.

Preparation of *Xenopus* extracts, membranes and cytosolic fractions
Cell free extracts from *Xenopus* eggs were prepared according to methods described by Hutchison (Hutchison, 1994). NEP-A, NEP-B and membrane-free cytosol were prepared as described previously (Drummond et al., 1999).

Immunoblotting and immunofluorescence on XTC cell lines.
XTC cell lines were grown and prepared for immunofluorescence and immunoblotting according to methods described by Drummond and colleagues (Drummond et al., 1999).

Nuclear assembly using the *Xenopus* cell-free system
All nuclear-assembly reactions were performed at 21°C using unfractionated *Xenopus* egg extracts (25 μl for immunofluorescence and 100 μl for immunoblotting). Demembranated *Xenopus* sperm were added at a final concentration of 10^3/μl. Reactions were supplemented with an energy-regenerating system consisting of 2 mM adenosine triphosphate (ATP), 10 mM phosphocreatine (PC) and 50 μg/ml creatine phosphokinase (CPK).

Time-course study of NE assembly
Five nuclear assembly reactions were set up and incubated at room temperature for 0, 10, 20, 40 or 80 minutes. For fixation, 175 μl of EGS [ethylene glycol bis-(succinic acid *N*-hydroxysuccinimide ester)] were added to each sample, which was then incubated at 37°C for 30 minutes and kept on ice until all reactions had finished. 100 μl of each sample were loaded onto 300 μl SNIB (60 mM KCl, 15 mM Tris pH 7.5, 15 mM NaCl, 1 mM β-mercaptoethanol, 0.15 mM spermine, 0.5 mM spermidine) containing 30% sucrose and centrifuged at 4000 *g* for 10 minutes. Coverslips were processed for immunofluorescence with antibodies against NEP-A or NEP-B.

Effect of emerin peptides on NE assembly
Each bacterially expressed peptide was added to a typical nuclear assembly reaction at a concentration of 0.5 μM, 4 μM or 8 μM. Nuclei were allowed to assemble at room temperature for 80 minutes. 100 μl of each sample were layered over 300 μl of SNIB-30% sucrose in cytology chambers and centrifuged at 4000 *g* for 10 minutes onto coverslips, which were processed for indirect immunofluorescence with antibodies specific for FG-repeat nucleoporins (414), pre-pore nucleoporins (Nup107), NEP-A vesicles and NEP-B vesicles. Chromatin was visualised by DAPI mounted in Mowiol.

For immunoblotting analysis, 100 μl of samples were diluted to a volume of 1 ml with ice-cold extraction buffer and layered over 500 μl of SNIB-30% sucrose in Eppendorf tubes. Nuclei were pelleted at 4000 *g* for 10 minutes. Pellets were suspended in 10 μl 1× SDS sample buffer, boiled, analysed by SDS-PAGE and immunoblotted with mAb 414 or with antibodies against NEP-A and NEP-B.

Chromatin-binding ability of emerin peptides
Emerin peptides were incubated individually with either condensed or decondensed *Xenopus* sperm chromatin for 15-30 minutes at room temperature and fixed with 4% formaldehyde at 4°C for 10 minutes. Sperm decondensation was achieved by incubating sperm chromatin with Pfaller buffer (250 mM sucrose, 50 mM KCl, 2.5 mM MgCl₂ and 10 mM HEPES-NaOH, pH 7.4) containing polyglutamic acid at a concentration of 2 μg/μl for 30 minutes at room temperature. Samples were loaded onto cushions containing 300 μl SNIB-30% sucrose and centrifuged at 4000 *g* for 10 minutes. Coverslips were processed for indirect immunofluorescence with the NCL-emerin antibody (Novocastra). Chromatin was counter stained with DAPI.

feSEM and TEM
Ovaries were surgically removed from mature females and placed in Ringer solution. Small pieces of ovary were placed in Petri dishes in buffer A (83 mM KCl, 17 mM NaCl, 10 mM HEPES, 250 mM sucrose, 0.3 mM CaCl₂, pH 7.4). Silicon chips precoated with poly-L-lysine were placed near the oocytes in the same dish. All solutions were kept ice cold.

Xenopus oocytes in developmental stage 3-4 identified as light brown to brown oocytes with diameters of 480-500 μm and yolk oocytes of diameter ~1600 μm from stage VI were used. Nuclei were manually isolated from stages 3-4 and stage 6 oocytes using glass needles and gently and quickly separated (released) from the surrounding cytoplasm. Two to three isolated nuclei were transferred to a nearby silicon chip and their NEs carefully opened manually using the glass needle. Samples were fixed after isolation by adding fix solution (see below) directly to the chip in the Petri dish and then the chip was transferred to another Petri dish with fresh fix. Chips were transferred from dish to dish without drying by keeping a drop of the previous solution on the chip. Samples were fixed for 10 minutes in 2% glutaraldehyde, 0.2% tannic acid, buffer A pH 7.4 and 0.3 mM MgCl₂. Importantly, the elapsed time from nuclear

isolation to placing in fix was always 5-10 seconds or less. Fixed samples were postfixed for 30 minutes in 1% OsO_4, washed in double-distilled H_2O, stained for 20 minutes in 1% uranyl acetate, dehydrated in ethanol and critical point dried from CO_2 using Arklone (Arcton 112, ICI Chemicals, Runcorn, UK) as the transitional solvent. Specimens were then sputter coated with a 4 nm layer of chromium using an Edwards Auto 306 coating unit (Edwards Instruments, UK) with a cryo-pumped vacuum system and were examined at 30 kV in a Hitachi S5200 field emission in lens scanning electron microscope (feSEM).

For TEM, isolated GVs were fixed in 2% glutaraldehyde, 0.2% tannic acid buffer A pH 7.4 and 0.3 mM $MgCl_2$ overnight at 4ºC. All samples were washed in double-distilled H_2O and postfixed in 1% OsO_4 in double-distilled water, dehydrated and embedded in Agar 100 resin. Thin sections were cut, stained with uranyl acetate and lead citrate and examined in a Jeol-1220 (Japan) at 80 kV.

For feSEM analysis of sperm pronuclei, 25 μl of egg extract were mixed with 0.2 μl sperm chromatin and incubated for the indicated times at room temperature, with or without peptides added as appropriate. This was diluted with 175 μl EGS fix, which consists of 1 mM ethylene glycol disuccinate di(*N*-succinimidyl) ester (EGS) (from 100 mM stock in DMSO) in a 1:3-diluted extraction buffer (EB: 100 mM KCl, 20 mM HEPES pH 7.5, 5 mM $MgCl_2$, 2 mM β-mercaptoethanol) and incubated for 30 minutes at 36°C. 100 μl of this was layered onto 500 μl 30% sucrose in SNIB buffer (60 mM KCl, 15 mM Tris-HCl pH 7.5, 15 mM NaCl, 1 mM β-mercaptoethanol, 0.15 mM spermine, 0.5 mM spermidine) in a modified microfuge tube (Goldberg et al., 1997) and spun at 400 *g* for 10 minutes onto a silicon chip (Agar Scientific, Stansted, UK). The chip was then transferred to fix containing 80 mM Pipes-KOH pH 6.8, 1 mM $MgCl_2$, 2% paraformaldehyde, 0.25% glutaraldehyde for 10 minutes, washed briefly in 0.2 M sodium cacodylate pH 7.4 and transferred to 1% OsO_4 in 0.2 M sodium cacodylate pH 7.4 for 10 minutes. Samples were then dehydrated through an ethanol series and transferred to dry acetone, then critical point dried. Next, they were examined as soon as possible in a Hitachi S5200 field emission in lens scanning electron microscope at an accelerating voltage of 10 kV.

References

Antonin, W., Franz, C., Haselmann, U., Antony, C. and Mattaj, I. W. (2005). The integral membrane nucleoporin pom121 functionally links nuclear pore complex assembly and nuclear envelope formation. *Mol. Cell* **17**, 83-92.

Bodoor, K., Shaikh, S., Salina, D., Raharjo, W. H., Bastos, R., Lohka, M. and Burke, B. (1999). Sequential recruitment of NPC proteins to the nuclear periphery at the end of mitosis. *J. Cell Sci.* **112**, 2253-2264.

Buendia, B. and Courvalin, J. C. (1997). Domain-specific disassembly and reassembly of nuclear membranes during mitosis. *Exp. Cell Res.* **230**, 133-144.

Burke, B. and Ellenberg, J. (2002). Remodelling the walls of the nucleus. *Nat. Rev. Mol. Cell Biol.* **3**, 487-497.

Cohen, M., Feinstein, N., Wilson, K. L. and Gruenbaum, Y. (2003). Nuclear pore protein gp210 is essential for viability in HeLa cells and Caenorhabditis elegans. *Mol. Biol. Cell* **14**, 4230-4237.

Courvalin, J. C., Segil, N., Blobel, G. and Worman, H. J. (1992). The lamin B receptor of the inner nuclear membrane undergoes mitosis-specific phosphorylation and is a substrate for p34cdc2-type protein kinase. *J. Biol. Chem.* **267**, 19035-19038.

Drummond, S. P. and Wilson, K. L. (2002). Interference with the cytoplasmic tail of gp210 disrupts "close apposition" of nuclear membranes and blocks nuclear pore dilation. *J. Cell Biol.* **158**, 53-62.

Drummond, S., Ferrigno, P., Lyon, C., Murphy, J., Goldberg, M., Allen, T., Smythe, C. and Hutchison, C. J. (1999). Temporal differences in the appearance of NEP-B78 and an LBR-like protein during Xenopus nuclear envelope reassembly reflect the ordered recruitment of functionally discrete vesicle types. *J. Cell Biol.* **144**, 225-240.

Dumont, J. N. (1972). Oogenesis in Xenopus laevis (Daudin). I. Stages of oocyte development in laboratory maintained animals. *J. Morphol.* **136**, 153-179.

Foisner, R. and Gerace, L. (1993). Integral membrane proteins of the nuclear envelope interact with lamins and chromosomes, and binding is modulated by mitotic phosphorylation. *Cell* **73**, 1267-1279.

Franz, C., Walczak, R., Yavuz, S., Santarella, R., Gentzel, M., Askjaer, P., Galy, V., Hetzer, M., Mattaj, I. W. and Antonin, W. (2007). MEL-28/ELYS is required for the recruitment of nucleoporins to chromatin and postmitotic nuclear pore complex assembly. *EMBO Rep.* **8**, 165-172.

Gant, T. M., Harris, C. A. and Wilson, K. L. (1999). Roles of LAP2 proteins in nuclear assembly and DNA replication: truncated LAP2beta proteins alter lamina assembly, envelope formation, nuclear size, and DNA replication efficiency in Xenopus laevis extracts. *J. Cell Biol.* **144**, 1083-1096.

Gerace, L. and Blobel, G. (1980). The nuclear envelope lamina is reversibly depolymerized during mitosis. *Cell* **19**, 277-287.

Gerace, L. and Burke, B. (1988). Functional organization of the nuclear envelope. *Annu. Rev. Cell Biol.* **4**, 335-374.

Goldberg, M. W., Wiese, C., Allen, T. D. and Wilson, K. L. (1997). Dimples, pores, star-rings, and thin rings on growing nuclear envelopes: evidence for structural intermediates in nuclear pore complex assembly. *J. Cell Sci.* **110**, 409-420.

Gruenbaum, Y., Wilson, K. L., Harel, A., Goldberg, M. and Cohen, M. (2000). Review: nuclear lamins-structural proteins with fundamental functions. *J. Struct. Biol.* **129**, 313-323.

Hallberg, E., Wozniak, R. W. and Blobel, G. (1993). An integral membrane protein of the pore membrane domain of the nuclear envelope contains a nucleoporin-like region. *J. Cell Biol.* **122**, 513-521.

Harel, A., Chan, R. C., Lachish-Zalait, A., Zimmerman, E., Elbaum, M. and Forbes, D. J. (2003). Importin beta negatively regulates nuclear membrane fusion and nuclear pore complex assembly. *Mol. Biol. Cell* **14**, 4387-4396.

Harlow, L. and Lane, D. (1988). *Antibodies. A Laboratory Manual*. Cold Spring Harbor, NY: Cold Spring Harbor Laboratory Press.

Harris, C. A., Andryuk, P. J., Cline, S., Chan, H. K., Natarajan, A., Siekierka, J. J. and Goldstein, G. (1994). Three distinct human thymopoietins are derived from alternatively spliced mRNAs. *Proc. Natl. Acad. Sci. USA* **91**, 6283-6287.

Heald, R. and McKeon, F. (1990). Mutations of phosphorylation sites in lamin A that prevent nuclear lamina disassembly in mitosis. *Cell* **61**, 579-589.

Hetzer, M., Gruss, O. J. and Mattaj, I. W. (2002). The Ran GTPase as a marker of chromosome position in spindle formation and nuclear envelope assembly. *Nat. Cell Biol.* **4**, E177-E184.

Hutchison, C. J. (1994). The use of cell-free extracts of Xenopus eggs for studying DNA replication in vitro. In *The Cell Cycle: A Practical Approach* (ed. P. Fantes and R. Brookes), pp. 177-195. Oxford: IRL Press.

Hutchison, C. J. (2002). Lamins: building blocks or regulators of gene expression? *Nat. Rev. Mol. Cell Biol.* **3**, 848-858.

Kishimoto, T. (1999). Activation of MPF at meiosis reinitiation in starfish oocytes. *Dev. Biol.* **214**, 1-8.

Lang, C., Paulin-Levasseur, M., Gajewski, A., Alsheimer, M., Benavente, R. and Krohne, G. (1999). Molecular characterization and developmentally regulated expression of Xenopus lamina-associated polypeptide 2 (XLAP2). *J. Cell Sci.* **112**, 749-759.

Lin, F., Blake, D. L., Callebaut, I., Skerjanc, I. S., Holmer, L., McBurney, M. W., Paulin-Levasseur, M. and Worman, H. J. (2000). MAN1, an inner nuclear membrane protein that shares the LEM domain with lamina-associated polypeptide 2 and emerin. *J. Biol. Chem.* **275**, 4840-4847.

Mansfeld, J., Guttinger, S., Hawryluk-Gara, L. A., Pante, N., Mall, M., Galy, V., Haselmann, U., Muhlhausser, P., Wozniak, R. W., Mattaj, I. W. et al. (2006). The conserved transmembrane nucleoporin NDC1 is required for nuclear pore complex assembly in vertebrate cells. *Mol. Cell* **22**, 93-103.

Marshall, I. C. B. and Wilson, K. L. (1997). Nuclear envelope assembly after mitosis. *Trends Cell Biol.* **7**, 69-74.

Mattaj, I. W. (2004). Sorting out the nuclear envelope from the endoplasmic reticulum. *Nat. Rev. Mol. Cell Biol.* **5**, 65-69.

Peter, M., Nakagawa, J., Doree, M., Labbe, J. C. and Nigg, E. A. (1990). In vitro disassembly of the nuclear lamina and M phase-specific phosphorylation of lamins by cdc2 kinase. *Cell* **61**, 591-602.

Pfaller, R., Smythe, C. and Newport, J. W. (1991). Assembly/disassembly of the nuclear envelope membrane: cell cycle-dependent binding of nuclear membrane vesicles to chromatin in vitro. *Cell* **65**, 209-217.

Ryan, K. J., Zhou, Y. and Wente, S. R. (2007). The karyopherin Kap95 regulates nuclear pore complex assembly into intact nuclear envelopes in vivo. *Mol. Biol. Cell* **18**, 886-898.

Rzepecki, R., Bogachev, S. S., Kokoza, E., Stuurman, N. and Fisher, P. A. (1998). In vivo association of lamins with nucleic acids in Drosophila melanogaster. *J. Cell Sci.* **111**, 121-129.

Schirmer, E. C., Florens, L., Guan, T., Yates, J. R., 3rd and Gerace, L. (2003). Nuclear membrane proteins with potential disease links found by subtractive proteomics. *Science* **301**, 1380-1382.

Sheehan, M. A., Mills, A. D., Sleeman, A. M., Laskey, R. A. and Blow, J. J. (1988). Steps in the assembly of replication-competent nuclei in a cell-free system from Xenopus eggs. *J. Cell Biol.* **106**, 1-12.

Smith, L. D., Xu, W. L. and Varnold, R. L. (1991). Oogenesis and oocyte isolation. *Methods Cell Biol.* **36**, 45-60.

Smythe, C., Jenkins, H. E. and Hutchison, C. J. (2000). Incorporation of the nuclear pore basket nup153 into nuclear pore structures is dependent upon lamina assembly: evidence from cell-free extracts from Xenopus eggs. *EMBO J.* **19**, 3918-3931.

Stavru, F., Nautrup-Petersen, G., Cordes, V. C. and Gorlich, D. (2006a). Nuclear pore complex assembly and maintenance in POM121- and gp210-deficient cells. *J. Cell Biol.* **173**, 477-483.

Stavru, F., Hulsmann, B. B., Spang, A., Hartmann, E., Cordes, V. C. and Gorlich, D. (2006b). NDC1: a crucial membrane-integral nucleoporin of metazoan nuclear pore complexes. *J. Cell Biol.* **173**, 509-519.

Vigers, G. P. A. and Lohka, M. J. (1991). A distinct vesicle population targets membranes and pore complexes to the nuclear envelope in Xenopus eggs. *J. Cell Biol.* **112**, 545-556.

Vigers, G. P. A. and Lohka, M. J. (1992). Regulation of nuclear envelope precursor functions during cell division. *J. Cell Sci.* **102**, 273-284.

Walther, T. C., Fornerod, M., Pickersqill, H., Goldberg, M., Allen, T. D. and Mattaj, I. W. (2001). The nucleoporin Nup153 is required for nuclear pore basket formation,

nuclear pore complex anchoring and import of a subset of nuclear proteins. *EMBO J.* **20**, 5703-5714.

Walther, T. C., Askjaer, P., Gentzel, M., Habermann, A., Griffiths, G., Wilm, M., Mattaj, I. W. and Hetzer, M. (2003a). RanGTP mediates nuclear pore complex assembly. *Nature* **424**, 689-694.

Walther, T. C., Alves, A., Pickersgill, H., Loiodice, I., Hetzer, M., Galy, V., Hulsmann, B. B., Kocher, T., Wilm, M., Allen, T. et al. (2003b). The conserved Nup107-160 complex is critical for nuclear pore complex assembly. *Cell* **113**, 195-206.

Ward, G. E. and Kirschner, M. W. (1990). Identification of cell cycle-regulated phosphorylation sites on nuclear lamin C. *Cell* **61**, 561-577.

Worman, H. J., Yuan, J., Blobel, G. and Georgatos, S. D. (1988). A lamin B receptor in the nuclear envelope. *Proc. Natl. Acad. Sci. USA* **85**, 8531-8534.

Wozniak, R. W., Bartnik, E. and Blobel, G. (1989). Primary structure analysis of an integral membrane glycoprotein of the nuclear pore. *J. Cell Biol.* **108**, 2083-2092.

Ye, Q. and Worman, H. J. (1996). Interaction between an integral protein of the nuclear envelope inner membrane and human chromodomain proteins homologous to Drosophila HP1. *J. Biol. Chem.* **271**, 14653-14656.

Zhang, C. and Clarke, P. R. (2001). Roles of Ran-GTP and Ran-GDP in precursor vesicle recruitment and fusion during nuclear envelope assembly in a human cell-free system. *Curr. Biol.* **11**, 208-212.